# Sensitivity of Repolarization Gradients to Infarct Borderzone Properties Assessed with the Ten Tusscher and Modified Mitchell-Schaeffer Model

# Sensitivity of Repolarization Gradients to Infarct Borderzone Properties Assessed with the Ten Tusscher and Modified Mitchell-Schaeffer Model

Justina Ghebryal[1(✉)], Evianne Kruithof[1], Matthijs J. M. Cluitmans[2,3], and Peter H. M. Bovendeerd[1]

[1] Cardiovascular Biomechanics, Biomedical Engineering Department, Eindhoven University of Technology, Eindhoven, The Netherlands
u.ghebryal@tue.nl
[2] Philips Research Eindhoven, Eindhoven, The Netherlands
[3] Maastricht University Medical Center, Maastricht, The Netherlands

**Abstract.** Post-infarction ventricular tachycardia (VT) is an important clinical problem that is often caused by a re-entrant circuit located in the infarct border zone (BZ). The main changes in the BZ are in action potential duration (APD) and conduction velocity (CV), which introduce high repolarization time gradients (RTGs) and can lead to re-entry. Computational models can help in VT-risk analysis. However, the complexity of these models and the representation of the electrophysiological properties of the BZ still require investigation. In this study we conduct a sensitivity analysis in which we apply changes in APD and CV in a BZ using the detailed biophysical Ten Tusscher (TT2) model and the phenomenological modified Mitchel-Schaeffer ($m$MS) ionic model. First, the effect of spatial discretization on the CV is compared for both models. The TT2 model showed much larger mesh dependency for the computed CV than the $m$MS model. Next, we propose a tuning method to match the $m$MS AP shape to the TT2 AP shape. We then compare APD restitution properties. The tuned $m$MS showed similar APD restitution properties for large diastolic intervals (DI), but started to deviate when decreasing the DI. Finally, for both the TT2 and tuned $m$MS model we found that RTG is more sensitive to variation in APD than to variation in CV. When varying the APD, differences between both models were more pronounced for short than for large APDs.

**Keywords:** Cardiac Electrophysiology · Border Zone · Sensitivity Analysis

## 1 Introduction

Ventricular tachycardia (VT) is a life-threatening arrhythmia that occurs frequently in patients that have previously suffered from myocardial infarction [6].


O. Bernard et al. (Eds.): FIMH 2023, LNCS 13958, pp. 147–156, 2023.
https://doi.org/10.1007/978-3-031-35302-4_15

Clinical and experimental studies show that VT is often caused by a re-entrant wave in the infarct border zone (BZ) [10], which is a region constituting the transition between the infarct scar and healthy myocardium. Ablation is a common procedure to isolate re-entry pathways across the BZ that are responsible for VTs [9]. However, identification of critical parts of the VT re-entry circuit for ablation in the clinic is still challenging [11]. Computational models offer a powerful research tool that can provide guidance in the ablation procedure, as such models may allow to test different ablation strategies. However, the question remains how to represent the BZ in computational models [10], and how to select the appropriate ionic model, considering the trade-off between model complexity and availability of patient-specific data to personalize model parameters.

Experimental data suggest that the most prominent changes of the BZ occur in action potential duration (ADP) and conduction velocity (CV), but they also show inconsistency and variations in the changes during the chronic and post-infarction phases [10]. The changes in APD and CV both determine the spatial distribution of repolarization times (RTs) in cardiac tissue. Subsequently, regional differences in RTs yield local RT gradients (RTG). This may promote re-entry through unidirectional block [1], which can form the basis for the occurrence of VTs. In computational models, a commonly used model for the description of ionic transport across the membrane is the detailed biophysical Ten Tusscher ionic model (TT2, consisting of 19 variables and 48 parameters) [18]. As an alternative, the phenomenological modified Mitchell-Schaeffer model ($m$MS, consisting of 2 variables and 5 parameters) has been proposed [3]. While the TT2 model has the advantage of a more detailed description of the underlying physics, the $m$MS model has the advantage of a more unique translation of changes in APD and CV to model parameter modifications.

Our goal is to study whether the phenomenological $m$MS model can show comparable behavior as the biophysical TT2 model in studying VT-risk. First, we study the effect of spatial discretization for both ionic models. Next, a tuning method is proposed in which we aim to match the shape of the AP of $m$MS to the one of TT2. Finally, we conduct a comparison of the tuned $m$MS model with TT2 on two different levels: (i) restitution properties for APD in a 1D-cable, and (ii) RTGs in a 2D-model with an idealized infarct scar and BZ where variations in APD and CV are applied. With these model comparisons, we aim to give more insights on computational model choice and its influence on VT-risk analysis.

## 2 Methods

The Cardiac Arrhythmia Research Package (CARP) was used to simulate electrical activity at tissue level [20] for both ionic models. For our simulations, a monodomain representation was solved using the finite element method.

### 2.1 Spatial Discretization Comparison

A 1D-cable is considered with spatial resolution represented by tetrahedral element size $\Delta x$ (Fig. 1**A**). Using the automatic parameterization approach [4], we

set the longitudinal conductivity ($\sigma_L$) constant, leading to CV = 0.6 m/s for $\Delta x$ = 100 µm. Next, a planar stimulus is applied at the left boundary of the mesh, which initiates propagation in x-direction. For our analysis, we varied the element resolution and computed the corresponding CVs for both ionic models.

### 2.2 AP Tuning

We propose a method to adjust the parameters of the original $m$MS model to match the AP shape to that of the TT2 model, allowing for comparison of RTG outcomes of both models when the AP is matched. Since the AP may differ for single-cells and tissue [17], we create matching APs in a 1D-cable (same setup as in Sect. 2.1). For the optimization process, $\tau_{close}$ in the $m$MS model is modified, as it has the most pronounced effect on the APD of and does not affect the CV [15]. In the original model $\tau_{close}$ is set to 150 ms. Next, we normalize the membrane voltage for both models between 0 and 1. To fit the main features of the cardiac AP, four different time instants are defined to be matched for both models:

$$T1 = t\left(\frac{dv}{dt}_{max}\right) \quad T2 = t\left(\frac{dv}{dt}_{min}\right) \quad T3 = t\left(APD_{50}\right) \quad T4 = t\left(APD_{90}\right) \tag{1}$$

$T1$ defines the time of the maximum time derivative of the first phase of the AP and expresses the moment of activation; $T2$ represents the time instant of the minimum time derivative for the last AP phase; and finally $T3$ and $T4$, depict APD at 50% and 90% of the repolarization, respectively. The time instants $T_{1,2,3,4}$ are visualized in Fig. 1**D**. We then minimize the following cost function $J$, which is defined as the normalized root squared mean error (NRMSE):

$$J(\tau_{close}) = \text{NRMSE} = \sqrt{\sum_{i=1}^{N} w_i \left(\frac{T_i - \tilde{T}_i}{N}\right)^2} \tag{2}$$

where $T_i$ is the duration in time for each of the four different ($N$ = 4) time instants for $m$MS, and $\tilde{T}_i$ the time instant for event $i$ in TT2. $w_i$ is a weight that is assigned to scale the error on the different time points. $w_{1,2,3}$ is set equal to 1 and $w_4$ to 2, as the main goal is to match the APD (best depicted by T4).

### 2.3 Restitution Properties

To compare the APD restitution properties of the tuned $m$MS and TT2, we use the S1-S2 protocol. The protocol consists of 20 stimuli at cycle length (CL) = 500 ms until a steady-state AP is reached; after that, CL is decreased in steps of 5 ms. The restitution curves (RCs) are obtained by plotting the steady-state APD against the diastolic interval (DI). Additionally, the slope of the APD RC is investigated, as it has been shown that a RC slope > 1 can promote conduction block and lead to re-entry [7].

### 2.4 Sensitivity to BZ Properties

For the sensitivity to BZ variability, we followed a similar simulation setup as proposed by Costa et al. [10]. Our simulation setup is given in Fig. 1**B**. The conductivity in the scar zone was set to approximately zero. To yield a velocity of respectively 0.6 and 0.4 m/s in the longitudinal and transversal direction, the conductivities were set using the automatic parameterization approach [4]. The tissue was stimulated 40 times with CL = 1000 ms to reach steady-state. A time step of $dt = 20$ µs is used to solve the monodomain equation.

**BZ Variability.** CV and APD are varied in the BZ in a realistic range as previously reported from experimental data [2,5,10]. For sensitivity to CV, the standard transversal conductivity ($\sigma_{T_n}$) that yields 0.4 m/s [4] was modified (Fig. 1**C**). For variations in APD we followed the AP tuning method described in Sect. 2.2 at CL = 1000 ms. First, the *m*MS model was tuned to TT2 by setting $\tau_{close}$ to 189 ms, referred to as the normal APD (indicated by the black line in Fig. 1**D**). Next, the duration of the normal APD is varied. For TT2, we modified the parameter $g_{Ks}$, as this has the most effect on APD for this ionic model [10]. Discrete variations were applied for the parameters $g_{Ks}$ and $\tau_{close}$. The resulting APs are shown in Fig. 1**D**. The maximum difference between the action potentials of both models corresponds to an NRMSE of 5.7 ms.

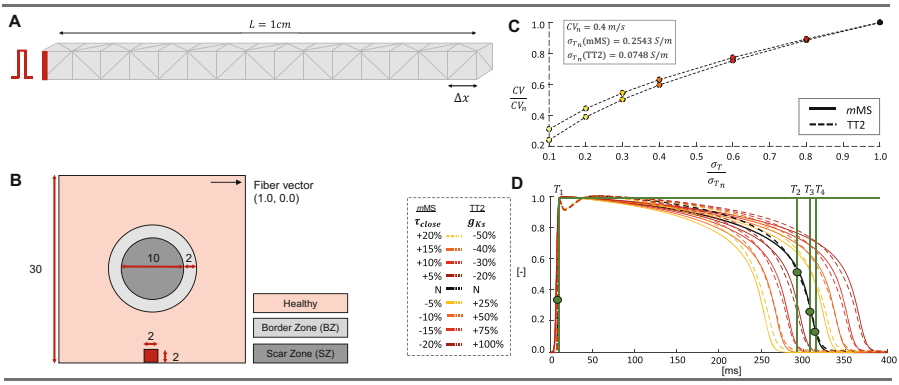


**Fig. 1. A:** 1D-cable with element size $\Delta x$ and length ($L$) 1 cm. **B:** Schematic 2D-tissue setup, dimensions given in mm. **C:** variations of the transversal conductivity $\sigma_T$, with reference $CV_n$ and $\sigma_{T_n}$ given in upper left box. **D:** APD variations around the normal (N) APD (indicated in black) for *m*MS (dotted line) by modifying $\tau_{close}$ and TT2 (solid line) by modifying $g_{Ks}$. Time instants $T_{1,2,3,4}$ are marked for the normal APD.

**Post-processing.** We computed the repolarisation time for *m*MS and TT2 as the time the AP reaches a threshold of 0.1 and −70 mV, respectively. The RTG was computed as the magnitude of the spatial gradient of the repolarization

time at each grid point. As a metric for RTG we compute (i) the surface area with RTG $\geq$ 3.5 ms/mm (SRTG), and (ii) the mean maximum RTG (mmRTG), defined as the mean of the 5% highest nodal RTG values (Fig. 2).

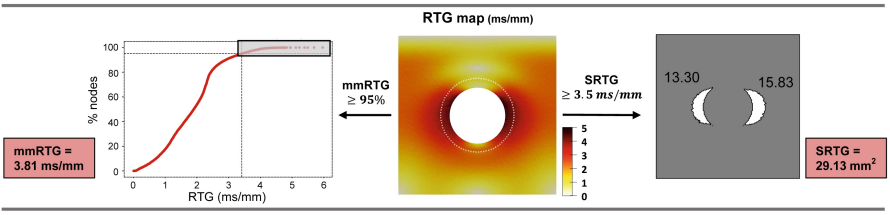


**Fig. 2.** Example for post-processing steps of the primary output of an RTG map. **SRTG:** surface RTG $\geq$ 3.5 ms/mm. **mmRTG:** mean maximal RTG computed as 5% highest nodal RTG values (highlighted box) from cumulative number of total nodes.

## 3 Results

### 3.1 Space-Discretization Analysis for the Conduction Velocity

Figure 3 shows the relationship between mesh resolution and CV. The TT2 ionic model exhibits a stronger dependency of CV on element size compared to $m$MS. Furthermore, it can be seen that for both the TT2 and $m$MS ionic models the solution for CV converges as the grid is refined. The deviation in CV increases about linearly with increasing element size, with a maximum deviation (for $\Delta x$ = 1000µm) of 0.040 m/s (−6.7%) and 0.364 m/s (−60.7%), for the $m$MS and the TT2 model, respectively.

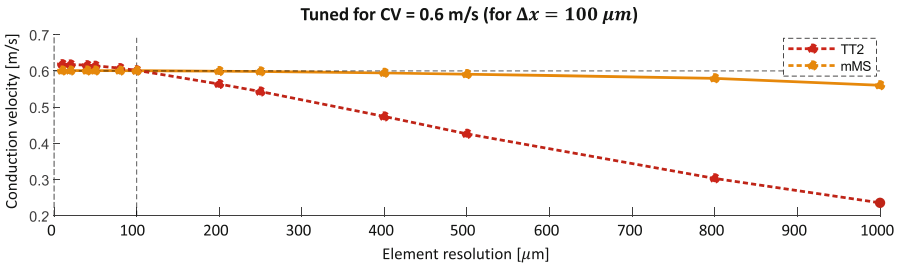


**Fig. 3.** Relationship of CV and element size with a constant conductivity. TT2: $\sigma_L$ = 0.1312 S/m and $m$MS: $\sigma_L$ = 0.5660 S S/m, resulting in CV = 0.6 m/s for $\Delta$x = 100 µm. (horizontal dotted line).

### 3.2 AP Tuning

For creating the RCs, the original $m$MS model was tuned at CL = 500 ms by a modification of $\tau_{close}$ = 192 ms (with NRMSE = 2.7 ms). For the 2D simulations, performed at CL=1000 ms, $J(\tau_{close})$ was minimized by a modification of $\tau_{close}$ to 189 ms with NRMSE = 1.9 ms.

### 3.3 Restitution Curves for APD

We constructed APD RCs for the original $m$MS, the tuned $m$MS, and the original TT2 ionic model. The results are given in Fig. 4**A**. The APD RCs for TT2 and tuned $m$MS are almost identical for a DI interval between 200–500 ms, but start to deviate at lower DIs. Although there are differences for small DIs, the tuned $m$MS does show better correspondence with TT2 than the original $m$MS. We also compared the magnitude of the APD slope (Fig. 4**B**). The time instant at which the RC slope exceeds 1, assumed to be indicative for VT risk, equals about 220 ms for the TT2 and the original $m$MS models. However, this is increased to about 235 ms in the $m$MS model.

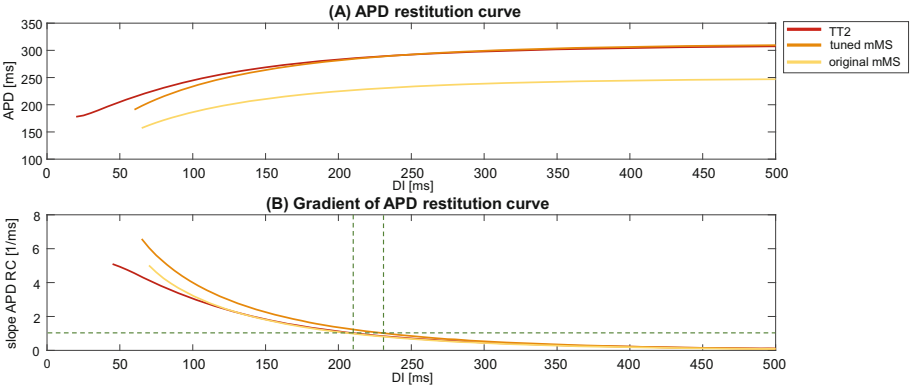


**Fig. 4. A:** APD restitution curves (RCs) for TT2 and the tuned and original $m$MS. **B**: The gradient of the APD RCs. The indicated green line shows the time instants for DIs where the gradients > 1. (Color figure online)

### 3.4 Repolarization Time Gradient

For the same variations in APD and CV, the tuned $m$MS and TT2 model showed qualitatively similar distribution patterns of repolarization gradients, with higher sensitivity to $\Delta$APD than $\Delta$CV (Fig. 5**A**–**D**). Quantitatively prolonging the APD shows approximately the same RTG metrics, but shortening of APDs show differences up to 180 mm$^2$ (for SRTG) and 3.0 ms/mm (for mmRTG) between both models (Fig. 5**E, F**). However, mmRTG also shows differences of approximately 2.0 ms/mm when prolonging the APD with slower CVs.

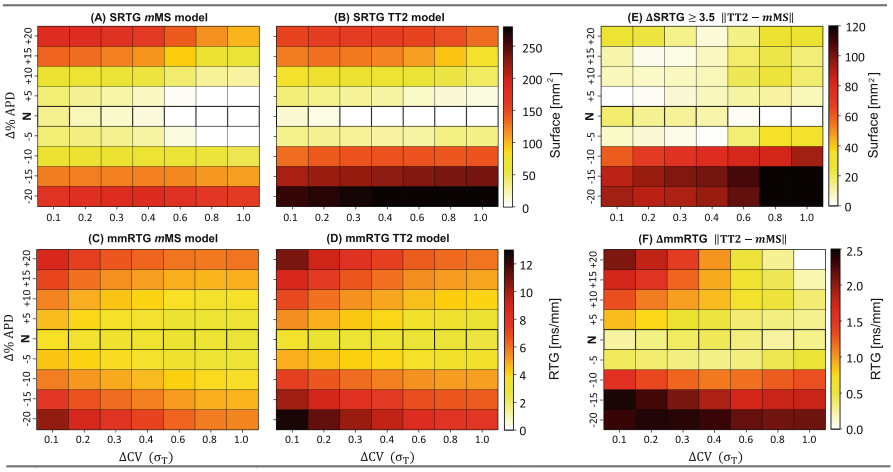


**Fig. 5.** Computed surface RTG $\geq$ 3.5 ms/mm (SRTG) and mean maximum RTG (mmRTG) for $m$MS and TT2 (**A**–**D**). Absolute difference in **(E)** SRTG and **(F)** mmRTG of the $m$MS and TT2 model

## 4 Discussion

First, we found that sensitivity of CV to element size is much higher in the TT2 model than in the $m$MS model. Normally, element sizes between 250 and 400 µm are used for whole heart simulations [13], with errors up to 10% considered acceptable [12]. For 400 µm, $m$MS and TT2 showed an underestimation of approximately 3% and 20%, respectively. Usually, this error in CV is compensated for by tuning the conductivity [4]. However, this conductivity tuning becomes complicated in unstructured meshes in whole heart geometries, suggesting that the use of the $m$MS model is more appropriate. We note that an important aspect in modeling EP is the requirement of high mesh resolution to capture the fast upstroke in time. This fast upstroke is related to the smallest time scale in the ionic model, which is $\tau_{in}$ for $m$MS. Additional simulations (not shown here) indeed showed when decreasing $\tau_{in}$, the solution of CV becomes more dependent on the element resolution. This implies a relation between time and space scales, which needs to be better studied to understand the reason behind mesh sensitivity.

Next, a tuning method was proposed in which we aim to match the AP of $m$MS to TT2, by only adjusting $\tau_{close}$. Relan et al. showed that in terms of APD personalisation, tuning $\tau_{close}$ of the MS model showed small errors of approximately 2% compared to patient data [16]. In our study, the tuned $m$MS model shows a similar APD RC as TT2 at large DIs compared to the original $m$MS model. However, when the DI is decreased, differences arise in both the computed APD and the APD RC slope. This is critical, as the APD RC slope at these short DIs can be coupled to the moment in which a conduction block

can be induced, which can lead to re-entry [7]. On the other hand, the original $m$MS shows similar behavior for the APD RC slope as TT2.

Finally, for both the tuned $m$MS and TT2 model we found that the RTG is more sensitive to APD variations than to CV, which corresponds to the results in Costa et al. [10]. Prolonging the APD shows approximately the same SRTGs for both models, but shortening the APD lead to large differences. The same effect was observed for differences in mmRTG. Although the variations in APD were not all created by precisely minimizing $J(\tau_{close})$, the APD fits showed a high degree of comparability with errors less than 5.7 ms. Consequently, we expect similar trends in the results when matching the APs exactly. Overall, our results indicate that APD tuning of the $m$MS model to TT2 by adapting $\tau_{close}$ may lead to the same APDs, but can lead to differences in RTG measures. Given that steep RTGs are known to be linked to re-entry induction [1], the differences in RTGs for both models can lead to different conclusions on their correlation to cardiac arrhythmias. This is important to take into account, as model parameterization and model choice is crucial in patient-specific VT-risk predictions.

Overall, our results highlight the importance of carefully tuning the parameters involved in the ionic model. In future research, it can be considered to improve the tuning of the $m$MS model to the TT2 model by e.g. optimizing all four $m$MS time parameters and including restitution properties to the cost function $J$ (Eq. 2), while taking into account the effect of time and space scales.

**Limitations.** When creating the RCs, we noticed for decreasing DIs that the amplitudes of the TT2 and $m$MS APs decreased, and for TT2 the AP shapes were changed remarkably. These changes are an expected effect of faster activation rates [8]. The ionic channels need sufficient time to recover, and too short DIs may not allow for this [14]. From literature, we could not find a commonly accepted definition for the AP to propagate or not. We defined an AP to propagate AP when the second AP reached at least the threshold of 95% of the amplitude of the normal (first) AP. For TT2 this threshold was set to approximately 10 mV and for $m$MS 0.95 [-].

SRTG was computed as the surface with RTG $\geq$ 3.5 ms/mm, as this value is within the previously investigated range of RTGs that can lead to conduction block. Various studies have found different values for a minimum RTG for unidirectional block to occur. These RTG values varied between 3.0 and 10.0 ms/mm, depending on subject-specific properties and the used geometry in the computational model [19]. Even though the exact threshold value is unclear, we expect that changes in this value would not affect our conclusions on the differences between the $m$MS and the TT2 model.

## 5 Conclusion

In this study, we first showed that the computed CV for the $m$MS model is less dependent on the mesh resolution than for the TT2 ionic model. Next, we found

that the tuned $m$MS model approximated APD restitution curves of the TT2 model much better that the original $m$MS model. On the other hand, the slope of the APD RC for TT2 was approximated better by the original $m$MS, which is important in VT-risk analysis. Finally, both for the TT2 and the tuned $m$MS model we found that RTG is more sensitive to variation in APD than to variation in CV. This suggests that it is more important to accurately represent the EP properties in the BZ in terms of APD than in terms of CV. Quantitatively, differences in sensitivity of RTG to variation in APD between the two models were more pronounced for short than for large APDs in the BZ. Overall, our study provides more insights on the differences of using the biophysical TT2 and phenomenological $m$MS model, which can be used in deciding which model to select for VT-risk analysis.

## References


1. Cluitmans, M., et al.: Noninvasive detection of spatiotemporal activation-repolarization interactions that prime idiopathic ventricular fibrillation. Sci. Transl. Med. **13**(620), eabi9317 (2021)
2. Connolly, A., Bishop, M.: Computational representations of myocardial infarct scars and implications for arrhythmogenesis. Clin. Med. Insights: Cardiol. **10**, CMC-S39708 (2016)
3. Corrado, C., Niederer, S.: A two-variable model robust to pacemaker behaviour for the dynamics of the cardiac action potential. Math. Biosci. **281**, 46–54 (2016)
4. Costa, C., Hoetzl, E., Rocha, B., Prassl, A., Plank, G.: Automatic parameterization strategy for cardiac electrophysiology simulations. In: Computing in Cardiology 2013, pp. 373–376. IEEE (2013)
5. Dangman, K., Danilo Jr., P., Hordof, A., Mary-Rabine, L., Reder, R., Rosen, M.: Electrophysiologic characteristics of human ventricular and purkinje fibers. Circulation **65**(2), 362–368 (1982)
6. Deng, D., Prakosa, A., Shade, J., Nikolov, P., Trayanova, N.: Sensitivity of ablation targets prediction to electrophysiological parameter variability in image-based computational models of ventricular tachycardia in post-infarction patients. Front. Physiol. **10**, 628 (2019)
7. Hayashi, M., et al.: Ventricular repolarization restitution properties in patients exhibiting type 1 Brugada electrocardiogram with and without inducible ventricular fibrillation. J. Am. Coll. Cardiol. **51**(12), 1162–1168 (2008)
8. Jing, L., Agarwal, A., Chourasia, S., Patwardhan, A.: Phase relationship between alternans of early and late phases of ventricular action potentials. Front. Physiol. **3**, 190 (2012)
9. Lopez-Perez, A., Sebastian, R., Izquierdo, M., Ruiz, R., Bishop, M., Ferrero, J.: Personalized cardiac computational models: from clinical data to simulation of infarct-related ventricular tachycardia. Front. Physiol. **10**, 580 (2019)
10. Mendonca Costa, C., Plank, G., Rinaldi, C., Niederer, S., Bishop, M.: Modeling the electrophysiological properties of the infarct border zone. Front. Physiol. **9**, 356 (2018)
11. Prakosa, A., et al.: Personalized virtual-heart technology for guiding the ablation of infarct-related ventricular tachycardia. Nat. Biomed. Eng. **2**(10), 732–740 (2018)

12. Prassl, A., et al.: Automatically generated, anatomically accurate meshes for cardiac electrophysiology problems. IEEE Trans. Biomed. Eng. **56**(5), 1318–1330 (2009)
13. Quarteroni, A., Lassila, T., Rossi, S., Ruiz-Baier, R.: Integrated heart-coupling multiscale and multiphysics models for the simulation of the cardiac function. Comput. Methods Appl. Mech. Eng. **314**, 345–407 (2017)
14. Ravens, U., Wettwer, E.: Electrophysiological aspects of changes in heart rate. Basic Res. Cardiol. **93**(1), s060–s065 (1998)
15. Relan, J., et al.: Coupled personalization of cardiac electrophysiology models for prediction of ischaemic ventricular tachycardia. Interface Focus **1**(3), 396–407 (2011)
16. Relan, J., Sermesant, M., Delingette, H., Pop, M., Wright, G., Ayache, N.: Quantitative comparison of two cardiac electrophysiology models using personalisation to optical and MR data. In: 2009 IEEE International Symposium on Biomedical Imaging: From Nano to Macro, pp. 1027–1030. IEEE (2009)
17. Seemann, G., Carillo, P., Weiss, D.L., Krueger, M.W., Dössel, O., Scholz, E.P.: Investigating arrhythmogenic effects of the hERG mutation N588K in virtual human atria. In: Ayache, N., Delingette, H., Sermesant, M. (eds.) FIMH 2009. LNCS, vol. 5528, pp. 144–153. Springer, Heidelberg (2009). https://doi.org/10.1007/978-3-642-01932-6_16
18. Ten Tusscher, K., Panfilov, A.: Alternans and spiral breakup in a human ventricular tissue model. Am. J. Physiol.-Heart Circulatory Physiol. **291**(3), H1088–H1100 (2006)
19. Tran, D., Yang, M., Weiss, J., Garfinkel, A., Qu, Z.: Vulnerability to re-entry in simulated two-dimensional cardiac tissue: effects of electrical restitution and stimulation sequence. Chaos Interdisc. J. Nonlinear Sci. **17**(4), 043115 (2007)
20. Vigmond, E., Hughes, M., Plank, G., Leon, L.: Computational tools for modeling electrical activity in cardiac tissue. J. Electrocardiol. **36**, 69–74 (2003)